A CONSIDERATION OF SUPPORT ASYMMETRY IN AN AUTOMATIC BALL BALANCING SYSTEM

David Rodrigues*, Alan Champneys*, Mike Friswell and Eddie Wilson***Dept of Engineering Mathematics, **Dept of Aerospace Engineering
University of Bristol, BS8 1TR, UK.

Abstract

We present an analysis of a two-plane automatic balancing device for rigid rotors. Ball bearings, which are free to travel around a race, are used to eliminate imbalance due to shaft eccentricity or misalignment. Here we consider the effect that asymmetries such as support anisotropy have on the auto-balancing process. Stability diagrams show that the device is robust to the considered asymmetries when the rotation speeds are supercritical and the mass imbalance is small.

Key words

Applications, Nonlinear systems, Control of oscillations.

1 Introduction

An automatic ball balancer (ABB) is a device which reduces vibrations in rotating machinery by compensating for the mass imbalance of the rotor. The ABB consists of a series of balls that are free to travel around a race which is set at a fixed distance from the shaft. During balanced operation the balls find such positions that the principal axis of inertia is repositioned onto the rotational axis. Because the imbalance does not need to be determined beforehand ABB's are ideally suited to applications where the amount of imbalance varies with the operating conditions. For example, automatic balancers are currently used in optical disk drives, machine tools and washing machines.

The idea behind automatic balancing has been with us since the early part of the last century and the existence of a stable balanced steady state at rotation speeds above the first critical frequency has long been known [Thearle, 1932]. However, in some cases the ABB may not balance the system even when operating at supercritical rotation speeds [Chung and Ro, 1999]. The autobalancing concept has also been extended to include two-plane devices that can compensate for both shaft eccentricity and shaft misalignment [Hedaya and Sharp, 1977], see Fig 1. Misalignment induces tilting vibrations and so models based on a 4DOF rotor which include gyroscopic effects must be considered [Sperling *et al.*, 2002; Chung and Jang, 2003; Chao *et al.*, 2003]. In a previous study we use Lagrange's method and rotating coordinates to derive an autonomous set of governing equations [Rodrigues *et al.*, 2008]. A symmetric system is then considered and numerical continuation techniques are used to map out the stability boundaries of the balanced state in various parameter planes. The setup on a real machine is, however, usually asymmetric, for example the supports may be anisotropic or have different stiffnesses [Ryzhik *et al.*, 2004]. Here we shall extend our work by considering the effect of these asymmetries.

The rest of this paper is organised as follows. In section 2 we present and discuss the equations of motion for the ABB. The steady states of the system are considered in section 3, and we focus on using numerical bifurcation theory to investigate the effect that the physical parameters have on the stability of the balanced state. Finally, in section 4 we draw conclusions and discuss possible directions for future work.

2 Equations of Motion

The setup of the ABB is illustrated in Fig. 1, and is based on a rigid rotor which has been fitted with a two-plane automatic balancer. The rotor has mass M, moment of inertia tensor $diag[J_t, J_t, J_p]$, and is mounted on two compliant linear bearings which are located at S_1 and S_2. The automatic balancer consists of a pair

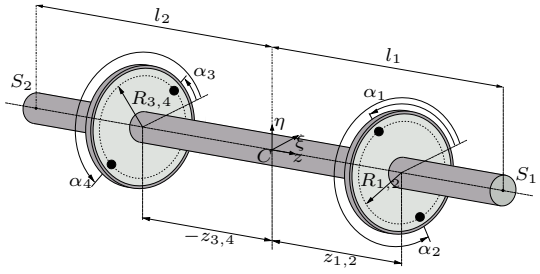

Figure 1. Schematic diagram of a two-plane automatic balancer.

of races that are set normal to the shaft in two separate planes. Each race contains two balancing balls of mass m_i, which move through a viscous fluid and are free to travel, at a fixed distance R_i from the shaft axis. The position of the ith ball is also specified by the axial and angular displacements z_i and α_i, which are written with respect to the $C\xi\eta z$ rotor axes.

For a fixed rotational speed Ω the equations of motion can be written in the inertial space frame as

$$\begin{aligned}&\begin{bmatrix}\mathbf{M} & \mathbf{0}\\ \mathbf{0} & \mathbf{M}\end{bmatrix}\ddot{\mathbf{x}}+\begin{bmatrix}\mathbf{C}_x & \Omega\mathbf{G}\\ -\Omega\mathbf{G} & \mathbf{C}_y\end{bmatrix}\dot{\mathbf{x}}+\begin{bmatrix}\mathbf{K}_x & \mathbf{0}\\ \mathbf{0} & \mathbf{K}_y\end{bmatrix}\mathbf{x}\\ &=\Omega^2\begin{bmatrix}\Re\left(\mathbf{f}_I e^{i\Omega t}\right)\\ \Im\left(\mathbf{f}_I e^{i\Omega t}\right)\end{bmatrix}\\ &\quad+\sum_{k=1}^{4}\begin{bmatrix}\dot{\varphi}_k^2\Re\left(\mathbf{f}_{b_k}e^{i\varphi_k}\right)+\ddot{\varphi}_k\Im\left(\mathbf{f}_{b_k}e^{i\varphi_k}\right)\\ \dot{\varphi}_k^2\Im\left(\mathbf{f}_{b_k}e^{i\varphi_k}\right)-\ddot{\varphi}_k\Re\left(\mathbf{f}_{b_k}e^{i\varphi_k}\right)\end{bmatrix},\end{aligned}\tag{1}$$

$$\begin{aligned}&m_kR_k^2\ddot{\varphi}_k+c_b\left(\dot{\varphi}_k-\Omega\right)\\ &=m_kR_k\left(\ddot{x}_k\sin\varphi_k-\ddot{y}_k\cos\varphi_k\right),\ k=1\ldots4.\end{aligned}\tag{2}$$

Here $\mathbf{x}=[x,\phi_y,y,-\phi_x]^{\mathrm{T}}$ is the vector of the rotor degrees of freedom,[1] $[x_k,y_k]=[x+z_k\phi_y,y-z_k\phi_x]$ are the race centre positions and $\varphi_k=\Omega t+\alpha_k$ are the angular displacements of the balls with respect to the non-rotating $Cxyz$ axes. The mass, gyroscopic, and damping and stiffness matrices in the x-direction are given respectively by

$$\mathbf{M}=\begin{bmatrix}M & 0\\ 0 & J_t\end{bmatrix}+\sum_{k=1}^{4}\begin{bmatrix}m_k & m_kz_k\\ m_kz_k & m_kz_k^2\end{bmatrix},\quad \mathbf{G}=\begin{bmatrix}0 & 0\\ 0 & J_p\end{bmatrix},$$
$$\mathbf{C}_x=\begin{bmatrix}c_{11} & c_{12}\\ c_{12} & c_{22}\end{bmatrix}\quad\text{and}\quad\mathbf{K}_x=\begin{bmatrix}k_{11} & k_{12}\\ k_{12} & k_{22}\end{bmatrix}.$$

Similar expressions can be written for $\mathbf{C}_y$ and $\mathbf{K}_y$, and the mass imbalance and ball vectors are given by

$$\mathbf{f}_I=\begin{bmatrix}M\epsilon e^{i\beta_1}\\ \chi\left(J_t-J_p\right)e^{i\beta_2}\end{bmatrix}\quad\text{and}\quad\mathbf{f}_{b_k}=\begin{bmatrix}m_kR_k\\ m_kR_kz_k\end{bmatrix}.$$

Here ϵ and χ are the rotor eccentricity and misalignment respectively and $\beta_{1,2}$ are the fixed phases of these imbalances with respect to the rotor ξ axis. Finally c_b is the viscous damping of the balls in the race as they move through the fluid. By taking $m_k=0$ in (1), we recover the equations of motion for a four degree of freedom rotor on anisotropic supports [Genta, 2005]. Note that we have used $-\phi_x$ instead of ϕ_x so that the equations take a more regular pattern and we have also implicitly assumed that the supports are orthotropic with the same axes of elasticity, namely x and y. Next, by setting the tilt angles $\phi_x=\phi_y\equiv0$, the system reduces to the equations of motion for the planar automatic balancer [Green *et al.*, 2006a]. If the supports are isotropic i.e $\mathbf{K}_x=\mathbf{K}_y$ and $\mathbf{C}_x=\mathbf{C}_y$, then the equations of motion can be made autonomous by transforming into the rotating frame. This aids the stability analysis of the steady states because circular whirls transform to fixed points. In previous studies we included the effect of geometric nonlinearities due to the inclinational rotor degrees of freedom ϕ_x and ϕ_y. However, by comparing stability charts and simulations we have found that these nonlinearities are negligible compared to those which are due to the ball angles α_i, hence, as is usual in rotordynamics, equation (1) is linearised with respect to the rotor coordinates. Finally we note that the effects of gravity and non constant spin speeds lie outside the scope of the present study, if interested we refer the reader to [Chung, 2005].

3 Stability of the Balanced Steady State

Steady state solutions are obtained by setting all time derivatives in the equations of motion (1-2) to zero. Moreover, if we also set the vibrational coordinates $\mathbf{x}=\mathbf{0}$, we arrive at the following condition for a balanced steady state

$$\mathbf{f}_I+\sum_{k=1}^{4}\mathbf{f}_{b_k}e^{i\alpha_k}=0.\tag{3}$$

Of course this equation simply states that the forces and moments acting on the rotor due to the imbalance and balancing balls must be in equilibrium. The solution is physically unique and exists provided that the balls have a mass large enough to cope with the imbalance. The ball positions $\boldsymbol{\alpha}=\boldsymbol{\alpha}^*$ can be determined in closed form but the equations are long and so are not presented here. Next we shall use the continuation package `AUTO` [Doedel *et al.*, 1997] to compute bifurcation diagrams of the full nonlinear system (1-2) which show the regions of stability of the balanced state (3) in various parameter planes. The boundaries of stability are formed by Hopf bifurcations which mark the onset of rotor vibrations.

For the remainder of this study we consider an ABB model with the following parameters

$$\begin{aligned}&M=1,\quad R_k=R=1,\quad k_{11}=1,\quad J_t=3.25,\\ &J_p=0.5,\quad l_1=-l_2=3,\quad z_{1,2}=-z_{3,4}=2,\\ &m_k=m,\quad \bar{c}_b\equiv\frac{c_b}{m}=0.01,\ \text{and}\quad c=0.02\\ &\text{where}\quad\mathbf{C}_x=c\mathbf{K}_x\quad\text{and}\quad\mathbf{C}_y=c\mathbf{K}_y.\end{aligned}\tag{4}$$

The first three constraints are simply rescalings which make the equations identical to the nondimensionalised

[1] As defined in [Genta, 2005]

version. The inertial parameter values are based on a solid cylindrically shaped rotor with a height of six times its radius. A rotating machine on compliant bearings with this geometry would typically undergo a two-plane balancing procedure before going into service.

When the stiffness and damping matrices have no off-diagonal terms the rotor's translational and inlinational degrees of freedom remain coupled, though only through the motion of the balancing balls. This situation can occur, for instance, in the case of a rigid rotor on two equal bearings with the center of mass exactly at the midspan. For the following stiffness matrices

$$\mathbf{K}_x = \mathbf{K}_y = \begin{bmatrix} 1 & 0 \\ 0 & 9 \end{bmatrix}, \tag{5}$$

the approximate critical frequencies for the cylindrical and conical whirls occur respectively at $\Omega_1 = \sqrt{\frac{k_{11}}{M}} = 1$ and $\Omega_2 = \sqrt{\frac{k_{22}}{J_t - J_p}} \simeq 1.81$.

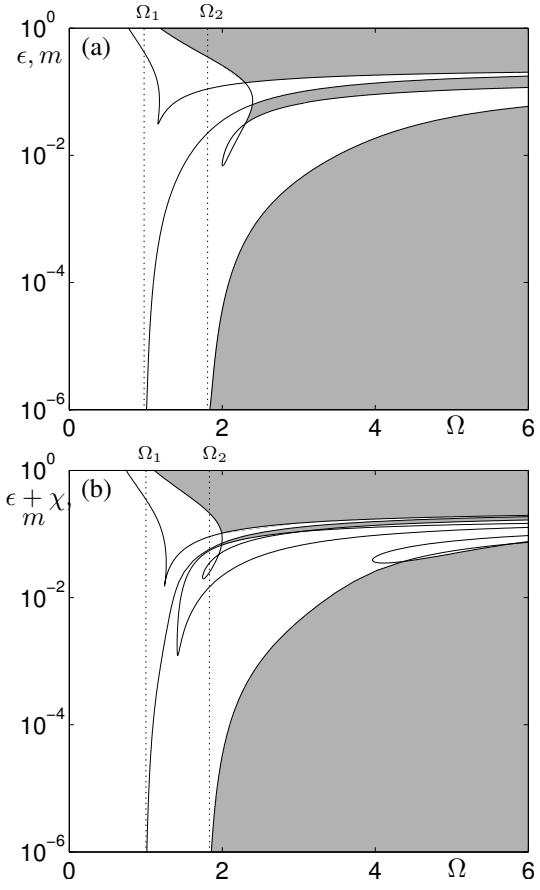

Figure 2. Panels (a) and (b) show stable regions of the balanced state (shaded) upon variation of the imbalance against Ω, whilst m is also varied so that $\boldsymbol{\alpha}^*$ remains constant. The vertical scale is logarithmic and the support parameters are given by equation (5).

Figure 2(a) shows the stability diagram for a static imbalance. The eccentricity ϵ, is plotted against Ω, whilst we also vary the ball mass so that $m = \epsilon$. Thus, the mass of the balls scales with the imbalance and the balanced state $\boldsymbol{\alpha}^*$ does not change value. A logarithmic scale is used for the vertical axis so that a wide range of eccentricities can be considered. The main area of interest for applications occurs where there is a large connected stable region for small eccentricities and supercritical rotation speeds. The Hopf curve which bounds this region asymptotes towards $\Omega = \Omega_2$ as $\epsilon \to 0$, hence there is no stable region in the subcritical regime. A similar plot is illustrated in Figure 2(b) for a dynamic imbalance case with $m = \epsilon + \chi,\ \epsilon = \chi$ and a constant phase $\beta_1 = 1$. Here we see that the regions of stability remain largely unchanged, however extra Hopf instability curves are present. These arise because the introduction of a small misalignment breaks the symmetry between the two races.

Next we consider the case where the stiffness matrices remain isotropic but have off-diagonal terms. This would occur, for example when the bearings have unequal stiffnesses or where the centre of mass is not at the midspan. We take

$$\mathbf{K}_x = \mathbf{K}_y = \begin{bmatrix} 1 & 3 \\ 3 & 45 \end{bmatrix}, \tag{6}$$

which yields $\Omega_1 \simeq 0.89$ and $\Omega_2 \simeq 4.07$, for the critical speeds linked with the cylindrical and conical whirls respectively. Figure 3(a) shows the results for a static imbalance and as Fig. 2, bifurcation curves asymptote to the critical frequencies as the ball mass and eccentricity tend to zero. The stable regions in the high eccentricity regimes have almost disappeared but more importantly the stable region for low eccentricities exists and has qualitatively the same shape as before. Finally we consider the case of anisotropic supports with stiffnesses

$$\mathbf{K}_x = \begin{bmatrix} 1 & 0 \\ 0 & 9 \end{bmatrix} \quad \text{and} \quad \mathbf{K}_y = \begin{bmatrix} 5 & 0 \\ 0 & 45 \end{bmatrix}. \tag{7}$$

Here the critical speeds for the translational and tilting modes in the x-direction are again $\Omega_{1_x} = 1$ and $\Omega_{2_x} \simeq 1.81$, and are $\Omega_{1_y} \simeq 2.24$ and $\Omega_{2_y} \simeq 4.05$ for the y direction. Figure 3(b) shows a 'brute force' bifurcation diagram for varying values of Ω, constant values of $m = \epsilon = 1 \times 10^{-4}$, and initial conditions where balls start on opposite sides of the race. This diagram was computed by running a simulation for each value of Ω, letting the transients die away and plotting the maximum values $\bar{A}_m$, of the average rotor vibration at points one unit length from the midspan. For all supercritical frequencies and at certain intervals between resonances the ABB (black curve) effectively eliminates rotor vibrations whereas for the plain rotor (grey curve) $\bar{A} \to \epsilon = 1 \times 10^{-4}$ as $\Omega \to \infty$. By contrast, the rotor fitted with an ABB performs far worse than one without when passing through the critical speeds. In fact at the first resonance the vibration level rises off the scale to a value of about 1×10^{-2}. In order to avoid these high

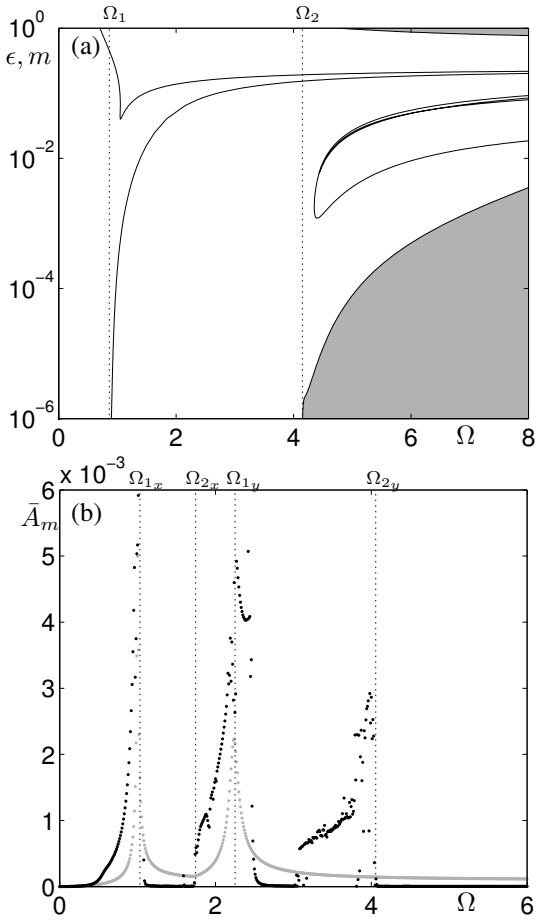

Figure 3. Panel (a) shows the stability chart for supports with stiffnesses given by equation (6) c.f. Fig. 2. Panel (b) is a bifurcation diagram where the rotor vibration $\bar{A}_m$ is plotted upon variation of Ω. The black (grey) curve is for the rotor with (without) an ABB.

vibration levels we envisage using a clamping mechanism in which the balls are fixed until supercritical rotation frequencies are reached [Thearle, 1932].

4 Conclusion

We have presented a simple model for a two-plane ABB for a rigid rotor on asymmetric supports. Stability charts obtained by numerical continuation of the Hopf bifurcation curves together with simulations show that the considered device can effectively eliminate imbalances arising from both shaft eccentricity and shaft misalignment. Furthermore, we have for the first time investigated the effects of support asymmetry and support anisotropy in the full nonlinear model, we show that they have little influence on the stable region provided that the machine is operating in the supercritical regime with typical values for the eccentricities[2] .

We plan to continue the present work by investigating the symmetry properties of the bifurcations which give rise to the balanced state. Normal form theory and the equivariant branching lemma can then be used to give explicit conditions for the stability of the bifurcating solutions. The transients of the system will be investigated through the use of pseudospectral techniques [Green *et al.*, 2006b] and experimental work is also in progress so that we may determine the influence of ball-race interactions, rotor flexibility and the performance of the autobalancer as it accelerates through the critical speeds.

[2]For machine tools and aircraft gas turbines $\epsilon \simeq 1 \times 10^{-5}$

5 Acknowledgements

The authors are grateful to Rolls-Royce plc. for financial support of this research.

References

Chao C.-P., Huang Y.-D., and Sung C.-K. (2003). Nonplanar dynamic modeling for the optical disk drive spindles equipped with an automatic balancer. *Mechanism and Machine Theory* **38** 1289-1305.

Chung J. and Ro D. S. (1999). Dynamic analysis of an automatic dynamic balancer for rotating mechanisms. *Journal of Sound and Vibration* **228**(5) 1035-1056.

Chung J. and Jang I. (2003). Dynamic response and stability analysis of an automatic ball balancer for a flexible rotor. *Journal of Sound and Vibration* **259**(1) 31-43.

Chung J. (2005). Effect of gravity and angular velocity on an automatic ball balancer. *Proc. IMechE Part C: J. Mechanical Engineering Science* **219** 43-51.

Doedel E., Champneys A. R., Fairgrieve T., Kusnetsov Y., Sanstede B. and Wang X. (1997). AUTO97: Continuation and bifurcation software for ordinary differential equations.

Genta G. (2005). *Dynamics of Rotating Systems*. Springer, New York.

Green K., Champneys A. R. and Lieven N. J. (2006a). Bifurcation analysis of an automatic dynamic balancer for eccentric rotors. *Journal of Sound and Vibration* **291** 861-881.

Green K., Champneys A. R. and Friswell M. I. (2006b). Analysis of the transient response of an automatic ball balancer for eccentric rotors. *International Journal of Mechanical Sciences* **48** 274-293.

Hedaya M. and Sharp R. (1977). An analysis of a new type of automatic balancer, *Journal of Mechanical Engineering Science* **19**(5) 221-226.

Rodrigues D. J., Champneys A. R., Friswell M. I. and Wilson R. E. (2008). Automatic two-plane balancing for rigid rotors. *International Journal of Nonlinear Mechanics* (In Press).

Ryzhik B., Sperling L. and Duckstein H. (2004). Autobalancing of anisotropically supported rigid rotors, *Technische Mechanik* **24** 37-50.

Sperling L., Ryzhik B., Linz Ch. and Duckstein H. (2002). Simulation of two-plane automatic balancing of a rigid rotor, *Mathematics and Computers in Simulation* **58** 351-365.

Thearle E. (1932). A new type of dynamic-balancing machine, *Transactions of the ASME* **54**(APM-54-12), 131-141.